AD NUMBER

AD490019

NEW LIMITATION CHANGE

TO

Approved for public release, distribution unlimited

FROM

Distribution authorized to U.S. Gov't. agencies and their contractors; Administrative/Operational Use; OCT 1952. Other requests shall be referred to David W. Taylor Model Basin, Washington, DC.

AUTHORITY

DTMB ltr, 4 Aug 1966

NAVY DEPARTMENT
THE DAVID W. TAYLOR MODEL BASIN
WASHINGTON 7, D.C.

WAVE EFFECTS IN ISOLATION MOUNTS

by

Mark Harrison, Alan O. Sykes, and
M. Martin

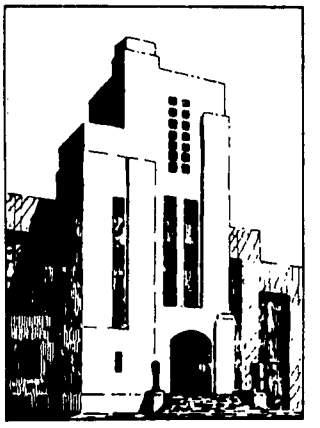

October 1952

Report 766

REVISED EDITION

TABLE OF CONTENTS

NOTATION

C	Phase velocity of a longitudinal elastic wave.
C_0	Phase velocity of a longitudinal elastic wave when the wavelength is much larger than the diameter of the elastic rod.
E	Young's modulus.
K	Stiffness of the mount.
l	Length of the mount.
M	Mass of the mounted machine.
m	Mass of the elastic material of the mount.
n	Dimensionless damping parameter $\omega\mu'/2E$
R	Lumped resistance of the mount.
R_c	Critical resistance.
S	Cross-sectional area of the mount.
T	Transmissibility.
u	Particle displacement in the elastic material.
v	Particle velocity in the elastic material.
Y	Admittance per unit length of the transmission line.
Z_0	Characteristic impedance of the transmission line.
α	Attenuation function.
β	Phase function.
γ	Propagation function.
μ	Shear viscosity of the mount material.
μ'	Longitudinal viscosity of the mount material $=4/3(1+\nu)\mu$
ν	Poisson's ratio.
ρ	Density of mount material.
σ_z	Longitudinal stress.
τ_{zy}	Shear stress.
ω	Angular frequency.
ω_0	Angular frequency at the spring mass resonance.
ω_i	Angular frequency at the standing wave resonances.

WAVE EFFECTS IN ISOLATION MOUNTS

by

Mark Harrison, Alan O. Sykes, and M. Martin

ABSTRACT

Both theoretical and experimental studies of wave effects in isolation mounts have been made. From the standpoint of vibration isolation, wave effects are important in the sense that the vibration isolating properties of a mount are changed by their presence. The well-known "lumped parameter" theory of vibration mounts predicts that the vibration isolation of a mount increases at 12 db per octave for frequencies well above the resonant frequency of the spring-mass system. This theory holds true only when the wavelength of the elastic wave in the mount is large compared to the dimensions of the mount. Standing waves occur, as would be expected, which in certain frequency ranges decrease the vibration isolation properties of the mount by as much as 20 db. For practical mounts, wave effects are most detrimental in the most audible frequency range (500 to 1000 cps). The theoretical and experimental treatments are in good agreement, and indicate various methods for improving the vibration isolation properties of the mount. Experimental data concerning isolation mounts fabricated of various materials are presented.

INTRODUCTION

If the performance of a typical isolation mount is measured, it is found that it departs from that which is predicted from simple vibration theory. This theory, which is based upon treating the spring, mass, and the resistance as lumped parameters, predicts that the vibration isolation of a mount increases at 12 db per octave for frequencies well above the resonant frequency of the spring-mass system. A detailed treatment of the lumped parameter theory will not be given in this paper, as it has been adequately presented in many texts on vibration engineering.[1] The performance of a mount in regard to vibration isolation is usually measured in terms of trans missibility, which is defined as the ratio of the force delivered by a mount to a base consisting of an infinite rigid mass to the force developed by the

---

[1]References are listed on page 22.

machine. In decibels, the transmissibility T, is given by

$$T = 20 \log_{10} \left(\frac{F_{base}}{F_{machine}} \right)$$

It is found experimentally that the transmissibility of an actual mount behaves in a manner that is illustrated in Figure 1. Reference 2 contains extensive data on many commercial isolation mounts, and these data all show that the transmissibility decreases at 12 db per octave for a limited frequency range only, while at higher frequencies a complicated behavior that is suggestive of standing waves is revealed.

It is the intention of this paper to explain the actual behavior of mounts in terms of wave effects. (The mounts will be treated as acoustic transmission lines with traveling and standing waves.) These waves are elastic, and for complicated mounts may be combinations of shear, compression, bulk, torsion, and Rayleigh surface waves. It may be seen from Figure 1 that wave effects have the ability to impair the noise isolation properties of the mount. It will be seen that standing waves can increase the transmissibility of a mount in certain frequency ranges by as much as 20 db above that which would be predicted from simple vibration theory. At higher frequencies, however, the transmissibility may be decidedly reduced.

The method of treating this problem has been both experimental and theoretical. On the experimental side, actual mounts have been constructed and their transmissibility measured. They are intended to be idealizations of compression mounts, though sufficiently similar to practical mounts to preserve the essential features. On the other hand, the mounts are sufficiently simplified to permit an adequate theoretical treatment without needless complications.

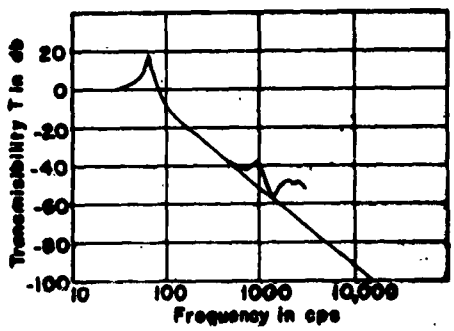

Figure 1 - Experimental Curve of Transmissibility T in db versus Frequency in cps

Lord Mount 200X FH90.
Machine mass 9.5 lb.

The agreement between theory and experiment is sufficiently good tc justify the principal thesis of the study, namely, that an adequate treatment can only be given by viewing the isolation mount as a continuous elastic structure in which wave motion occurs.

THEORETICAL DISCUSSION

Longitudinal wave motion in an elastic rod with viscous moduli and whose diameter is small compared to the wavelength is given by the equation[5]

$$\rho \frac{\partial^2 u}{\partial t^2} = E \frac{\partial^2 u}{\partial x^2} + \mu' \frac{\partial^3 u}{\partial t \partial x^2} \qquad [1]$$

Because of the finite cross section of the rod, there will be lateral motion and lateral stress, so this derivation is not exact. The effect of this approximation on the velocity and damping will be discussed in the Appendix.

Solutions of Equation [1] for the case of an elastic rod terminated at one end by an infinite rigid mass and with the other end excited by a simple harmonic driving force $F = F_0 e^{j\omega t}$ will now be investigated. For this case, Equation [1] becomes

$$\rho \frac{\partial^2 u}{\partial t^2} = (E + j\omega\mu') \frac{\partial^2 u}{\partial x^2} \qquad [2]$$

The solution to this equation is

$$u = A_1 e^{\gamma x} + A_2 e^{-\gamma x} \qquad [3]$$

where $\gamma = \alpha + j\beta$, the complex propagation function. If $\omega\mu'/E \ll 1$, then it may be verified by substitution that

$$\alpha = \frac{\omega^2 \mu'}{2\rho C_0^3} \qquad [4]$$

$$\beta = \frac{\omega}{C_0} \qquad [5]$$

$$C_0 = \left(\frac{E}{\rho}\right)^{1/2} \qquad [6]$$

An exact solution to the differential equation has been given by Nolle,[6] but it develops that for the amount of damping in the mount considered in this paper the error in using this approximate solution is negligible. The termination of the rod in the infinite rigid base, as shown in Figure 2, imposes the boundary condition $u = 0$ at $x = 0$. At $x = l$, $P = F_0/S$. Equation [3], when solved using these boundary conditions, gives two equations that lead to the two equations,

$$\frac{\partial u(x)}{\partial t} = \dot{u}(x) = \frac{F_0 \sinh \gamma x}{\frac{S}{l}\left[\mu' - \left(\frac{jE}{\omega}\right)\right] \gamma l \cosh \gamma l} \qquad [7]$$

$$p(x) = \frac{F_0 \cosh \gamma x}{S \cosh \gamma l} \qquad [8]$$

It is to be observed that the reciprocal of the admittance per unit length of the transmission line is given by

$$\frac{Z_0}{\gamma} = \frac{1}{y} = \left[\mu' - \left(\frac{jE}{\omega}\right)\right] \qquad [9]$$

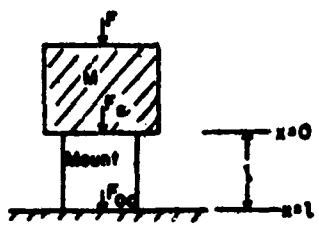

Figure 2 - Diagram of Isolation Mount and Acting Forces

For those who like analogies, the case here is one of an open circuited transmission line whose series impedance is an inductance and whose shunt impedance is a resistance in series with a capacity. In the present treatment, use will be made of the well-known formal identity of acoustic and electrical transmission line equations. In this point of view one merely needs to know γ and Z_0. The propagation function has already been found (Equations [4] and [5]), and the characteristic impedance Z_0 is known to be ρC_0.

All transmission line relationships given in the subsequent treatment are contained elsewhere.[5]

The isolation mount is represented in Figure 2. The relationships for the forces shown in the figure are

$$\frac{F_s}{F} = \frac{Z}{(Z + j\omega M)} \qquad [10]$$

$$\frac{F_{0x}}{F_0} = \frac{1}{\cosh \gamma l} \qquad [11]$$

where Z, the input impedance of the mount, is given by the equation,

$$Z = SZ_0 \coth \gamma l \qquad [12]$$

The ratio of F_{0x} to F is given by

$$T = \frac{F_{0x}}{F} = \frac{1}{\frac{j\omega M}{SZ_0} \sinh \gamma l + \cosh \gamma l} \qquad [13]$$

This ratio of forces F_{0_e}/F is defined as the transmissibility T for the mount.

It is instructive to observe that this gives the simple vibration theory for the mount when the wavelength of sound in the mount is much larger than the physical length of the mount. From Equation [9] it is seen that

$$Z_0 = \frac{\gamma}{y} = \gamma\left[\mu' - \left(\frac{jE}{\omega}\right)\right] \qquad [14]$$

Equation [13] can then be written

$$T = \frac{1}{\frac{j\omega M}{\frac{S}{l}\left[\mu' - \left(\frac{jE}{\omega}\right)\right]} \cdot \frac{\sinh \gamma l}{\gamma l} + \cosh \gamma l} \qquad [13a]$$

Now as $\lambda \gg l, \gamma l \to 0$, so that $\sinh \gamma l \to \gamma l$. The expression for T then becomes

$$T = \frac{R - \left(\frac{jK}{\omega}\right)}{R + j\left[\omega M - \left(\frac{K}{\omega}\right)\right]} \qquad [15]$$

where R and K have been defined by the equations,

$$R = \frac{\mu' S}{l}$$
$$K = \frac{ES}{l} \qquad [16]$$

These quantities are the ordinary resistance and stiffness of the mount that are used in vibration theory. The magnitude of T can be written in a convenient nondimensional form,

$$|T| = \left[\frac{1 + \left(\frac{2\omega R}{\omega_0 R_c}\right)^2}{\left\{1 - \left(\frac{\omega}{\omega_0}\right)^2\right\}^2 + \left(\frac{2\omega R}{\omega_0 R_c}\right)^2}\right]^{1/2} \qquad [17]$$

where $\omega_0 = (K/M)^{\frac{1}{2}}$, and $R_c = 2(KM)^{\frac{1}{2}}$. This equation is more adequately discussed in Reference 1.

For purposes of computation, Equation [13] can be put into other forms. In the discussion of vibration mounts, only the magnitude of T is of interest, so the following treatment is accordingly restricted. After no inconsiderable amount of algebra, the magnitude of Equation [13] can be written

$$|T|^2 = \frac{1 + 5n^2}{\{(1+5n^2)[\sinh^2 \alpha l + \cos^2 \beta l] + \left(\frac{\omega M}{\rho C_0 S}\right)^2 [\sinh^2 \alpha l + \sin^2 \beta l] + \left(\frac{\omega M}{\rho C_0 S}\right)[n \sinh \alpha l - 2(1+2n^2)\sin 2\beta l]\}} \qquad [18]$$

where n is the nondimensional damping parameter and is equal to $\omega\mu'/2E$.

It is instructive to examine Equation [18] when the viscous damping is zero. Setting $n = 0$ we obtain

$$|T| = \frac{1}{\left|\cos\beta l - \frac{\omega M}{\rho C_0 S}\sin\beta l\right|} \qquad [19]$$

It is convenient to introduce the following nondimensional quantities

$$n = \omega\mu'/2E$$

$$\beta l = \omega/\omega_0\,(m/M)^{1/2}$$

$$\alpha l = n\omega/\omega_0\,(m/M)^{1/2}$$

$$\omega M/\rho C_0 S = \omega/\omega_0\,(M/m)^{1/2}$$

where $m = \rho l S$, the mass of the elastic material in the isolation mount. Equations [18] and [19] then become

$$|T|^2 = \frac{1+5n^2}{\left\{\begin{array}{l}\left\{1+5n^2+\left[\frac{\omega}{\omega_0}\left(\frac{M}{m}\right)^{1/2}\right]^2\right\}\sinh^2\left[n\,\frac{\omega}{\omega_0}\left(\frac{m}{M}\right)^{1/2}\right]+n\,\frac{\omega}{\omega_0}\left(\frac{M}{m}\right)^{1/2}\sinh\left[2n\,\frac{\omega}{\omega_0}\left(\frac{m}{M}\right)^{1/2}\right] \\ \qquad +(1+5n^2)\cos^2\left[\frac{\omega}{\omega_0}\left(\frac{m}{M}\right)^{1/2}\right]+\left[\frac{\omega}{\omega_0}\left(\frac{M}{m}\right)^{1/2}\right]^2\sin^2\left[\frac{\omega}{\omega_0}\left(\frac{m}{M}\right)^{1/2}\right] \\ \qquad -\frac{\omega}{\omega_0}\left(\frac{M}{m}\right)^{1/2}(1+2n^2)\sin\left[2\,\frac{\omega}{\omega_0}\left(\frac{m}{M}\right)^{1/2}\right]\end{array}\right\}} \qquad [20]$$

$$|T| = \frac{1}{\left|\cos\left[\frac{\omega}{\omega_0}\left(\frac{m}{M}\right)^{1/2}\right]-\frac{\omega}{\omega_0}\left(\frac{M}{m}\right)^{1/2}\sin\left[\frac{\omega}{\omega_0}\left(\frac{m}{M}\right)^{1/2}\right]\right|} \qquad [21]$$

These are the forms that best lend themselves to discussions and computations. It is 20 log$T$, with T given by Equation [20], that is plotted in Figures 3 - 7, inclusive. The denominator of Equations [20] and [21] becomes a minimum when

$$\omega_i = \omega_0 i\pi\left(\frac{M}{m}\right)^{1/2}, \qquad i = 1, 2, 3\cdots \qquad [22]$$

The corresponding values of ω_i are the standing wave angular resonant frequencies. The denominator of Equations [20] and [21] becomes a minimum when $\omega/\omega_0(m/M)^{1/2}$ becomes small because of ω approaching ω_0. This gives the

ordinary vibration theory resonance.

It is of interest to write Equation [17] using a different notation. After considerable algebra the equation can be written

$$T = \left[\frac{1 + 4n^2 \left(\frac{\omega}{\omega_0}\right)^2}{\left\{1 - \left(\frac{\omega}{\omega_0}\right)^2\right\}^2 + 4n^2 \left(\frac{\omega}{\omega_0}\right)^2} \right]^{1/2} \qquad [23]$$

It should be noted that in this case n becomes identical with the ratio R/R_c that is introduced as a dimensionless parameter in the ordinary vibration theory. This can be shown directly by going back to the definitions of n, R, and R_c, and performing the necessary algebra. At the low frequency resonance, when damping is not too large, the expression for the transmissibility becomes approximately

$$T_0 = \frac{1}{2n_0} \qquad [24]$$

It is also of interest to point out that

$$n_0 = \frac{1}{2Q_0} \qquad [25]$$

where Q_0 is the Q at the low frequency resonance, and is defined by the equation $Q_0 = \omega_0 M/R_c$.

It may seem surprising that the mass ratio, M/m, turned out to be a fundamental parameter in the preceding treatment, so it seems appropriate to add a few words of explanation. Suppose that both the machine mass M and the low resonant angular frequency ω_0 are specified. Since $\omega_0 = (K/M)^{1/2}$, K is also specified. With K specified, it is still possible to make an independent choice of m. For example, if the mount is a circular cylinder, K, is given in terms of the area, length, and Young's modulus by the equation,

$$K = \frac{ES}{l} \qquad [26]$$

Keeping K and E constant still permits an arbitrary choice of S. By choosing S and l large or small, the value of m can be made large or small. The shape of the mount changes with the value of m since the linear dimensions of the mount do not remain proportional. In conjunction with these ideas, Equation [26] can be written

$$m = \frac{\rho E S^2}{K} \qquad [27]$$

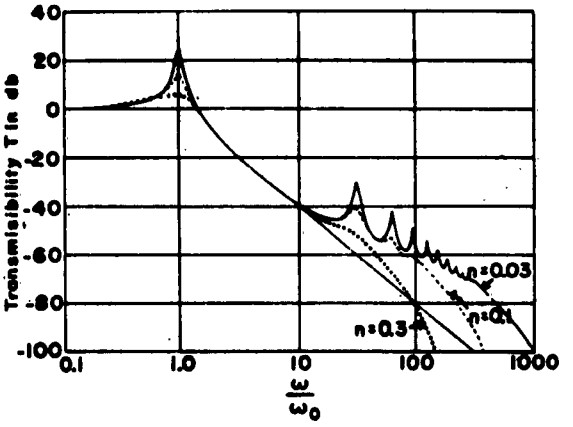

Figure 3 - Theoretical Curve of Transmissibility T in db versus Frequency Ratio ω/ω_0 for a Mass Ratio $M/m = 100$

where $\rho = m/Sl$. Thus it is seen that choosing K still leaves us free to choose m, and this is tantamount to choosing a shape for the mount.

Returning to the discussion of the theoretical curve of transmissibility, there is plotted in Figures 3 - 7, the transmissibility T versus the frequency ratio ω/ω_0 for a mass ratio M/m of 100 and for three values of the damping parameter, n: 0.03, 0.1, and 0.3. Most practical mounts have mass ratios between 100 and 1000, and values of n between 0.1 and 0.03. The previously mentioned curves are computed on the assumption both of constant velocity of the elastic wave in the mount and of constant n. This is only approximately true in actual mounts, but plotting the curves on this basis helps reveal the pertinent features..

In Figure 3 it is seen that the mount obeys the lumped parameter vibration theory until ω approaches standing wave frequencies. The transmissibility versus frequency curve then departs from the familiar 12-db per octave relationship. The standing wave frequencies can be computed by the approximate relationship,

$$\omega_i/\omega_0 = \pi i \left(\frac{M}{m}\right)^{1/2} \quad i = 1, 2, 3, \ldots,$$

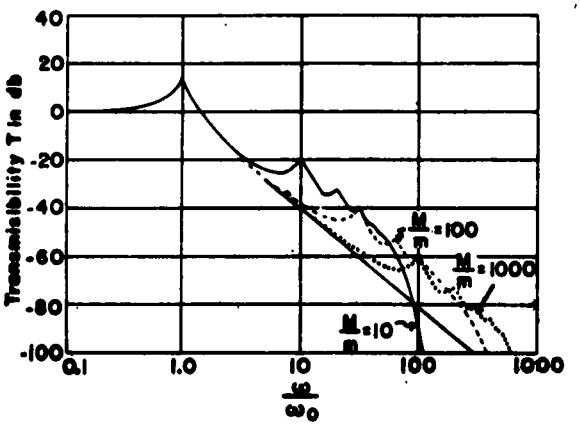

Figure 4 - Theoretical Curve of Transmissibility T in db versus Frequency Ratio ω/ω_0 for Damping Parameter $n = 0.1$ and for Various Mass Ratios

where ω_i is the angular frequency of the standing wave. The transmissibility T_i, at ω_i can be computed from the approximate relationship,

$$\frac{1}{T_i} = \frac{\omega_i}{\omega_0}\left(\frac{M}{m}\right)^{1/2} \sinh\left[n\,\frac{\omega_i}{\omega_0}\left(\frac{m}{M}\right)^{1/2}\right]$$

which is an approximation of Equation [20]. It is interesting to note that the peaks in the transmissibility because of the standing waves decrease at 12 db per octave and are displaced upward from the simple vibration theory curve by 20 log$n$. The valleys between the peaks decrease at 6 db per octave, and the standing waves are no longer discernible for frequency ratios above

the ratio where a line drawn through the peaks and valleys intersects. It can be shown that for these high frequency ratios the mount can be viewed as a dissipative medium in which the elastic waves are exponentially attenuated. In this frequency range the transmissibility decreases at an accelerated rate, as the figures clearly show.

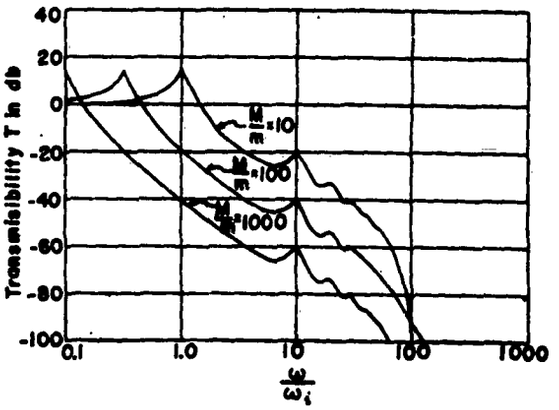

Figure 5 - Theoretical Curve of Transmissibility T in db versus Frequency Ratio ω/ω_i for Damping Parameter $n = 0.1$ and for Various Mass Ratios

Figure 3 illustrates the advantage of high damping. This is at variance with the simple vibration theory which states that high damping can increase the transmissibility. The discrepancy between the conclusions has its basis in the fact that simple vibration theory is only a partial description of the situation.

Figure 4 shows the transmissibility for various mass ratios, with the damping held constant. In this situation there does not appear to be a universally best mass ratio. The mass ratio that gives the best performance, i.e., the smallest transmissibility, in one frequency range may give poor performance in another frequency range.

In Figure 5 a comparison is made upon a different basis--the machine mass M is specified and the stiffness K and hence, the resonant frequency ω_0 is varied, since $\omega_0 = (K/M)^{1/2}$. However, K is varied by changing only the cross-sectional area of the mount and leaving the length of the mount constant. K is given in terms of the dimensions of the mount by the equation $K = E(S/l)$, where S is the cross-sectional area, l is the length, and E is Young's modulus. In the figures, the transmissibility in decibels is plotted versus the dimensionless frequency ratio ω/ω_i, where ω_i is the angular frequency of the first standing wave. The results lead to the same conclusion as does the simple vibration theory, namely, that ω_0 should be as low as possible to give low transmissibility at high frequencies. Figure 6 results

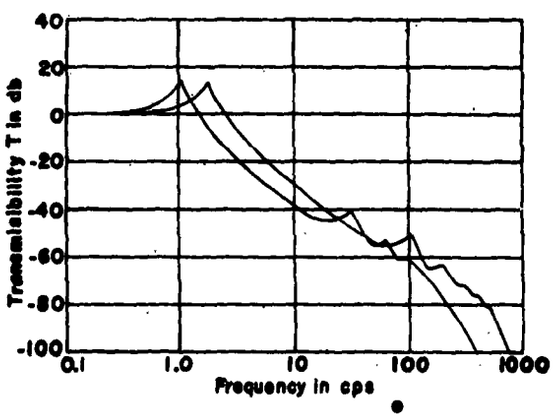

Figure 6 - Theoretical Curve of Transmissibility T in db versus Frequency for Damping Parameter $n = 0.1$ and Two Mass Ratios Differing by a Factor of 3

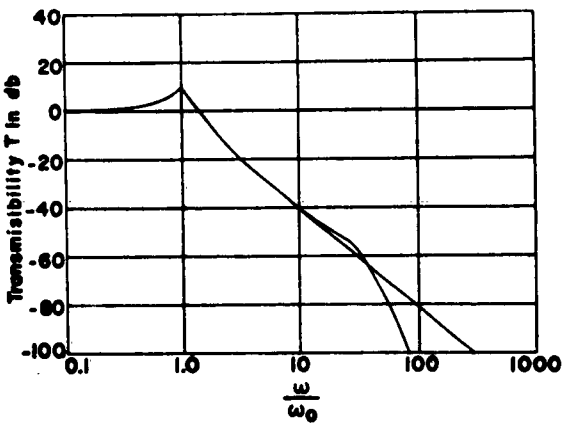

Figure 7 - Theoretical Curve of Transmissibility T in db versus Frequency Ratio ω/ω_0 for a Mount Constructed of Buna

The mass ratio M/m = 100 and f_0 = cps.

from the same conditions that were observed in Figure 5, except that the stiffness is changed by varying the length of the mount rather than the cross-sectional area. An arbitrary frequency scale is used since there are no convenient dimensionless frequency parameters. The stiffness for the two curves differs by a factor of three. The standing wave frequencies, ω_i, vary inversely with the length of the mount, while the low resonant frequency, ω_0, varies inversely with the square root of the length. The conclusion indicated here once again is that it is advantageous to have ω_0 as low as possible.

In Figure 7 the theoretical curve is given for a mount constructed of Buna-*N* cement. The data for this were obtained from Reference 4. This curve is included because Buna-*N* has remarkably good properties with respect to the amount of damping, and the effects of standing waves are negligible. In fact, the transmissibility is less than simple vibration theory would lead one to expect.

EXPERIMENTAL RESULTS

The types of mounts which were studied experimentally were compressional and of cylindrical form. One spring mount was considered to show that the method of analysis used was applicable. There were various reasons for choosing a particular shape of mount and the material from which the mount was fabricated. Actual compression mounts have complicated shapes and often operate with complicated constraints on the boundaries. As such, they present an impossibly difficult analytical problem. A circular cylinder with its ends bonded to the metal disks was chosen because if it became necessary to obtain an analytical solution to the elasticity problem, it would be possible to do so. Actually, it has not yet appeared imperative to obtain the exact solution to the elastic problem, though it does appear desirable. In this study the analytic problem has been circumvented by using cylinders of different length to diameter ratios. If the length of the cylinder is considerably larger than the diameter, then the stress distribution is plane over a cross section sufficiently distant from the constraint on the ends which results from the rubber-metal bond. Conditions are ideally simplified

in this case, and the theoretical results apply to an excellent degree of approximation, since the elastic properties of the cylinder are uniform throughout most of its length. Here, for example, the stiffness K, is quite accurately related to Young's modulus E by $K = ES/l$, where S and l are the cross section and length of the cylinder, respectively. If, however, the length of the cylinder is considerably smaller than the diameter, then the effect of constrained ends is to complicate the stress and strain distribution near the ends of the cylinder. This results in velocity and damping changes in the mount material. Also, if one attempts to compute K as indicated above he would use, instead of E, some effective modulus which is a function of S/l. This function can be obtained analytically or experimentally. This effect of the constrained ends is called the "end effect" and is discussed in the Appendix.

The mounts were all tested with a low value of mass ratio, M/m, since for large mass ratios the transmissibility becomes small at relatively low frequencies and difficulty with noise pick-up is encountered. For large mass ratios, there is no reason to expect the mount to behave in a manner different from that predicted by theory. It is expected, however, that the effective stiffness of the mount will change with different loads, since the static stress-strain curve is not quite linear.

The mounts were constructed from conveniently available materials. Some of the materials were rubber with ordinary elastic and damping constants, corprene, cell-tight rubber, and a steel helical spring. These materials were chosen because it was believed that their unusual physical properties would exaggerate various effects and provide a test for the applicability of the theoretical ideas.

Table 1 gives the physical dimensions of the cylindrical mounts, their mass m, and the designation by which the mounts are referred to in the figures. The numerical designation refers to a kind of material, and the alphabetical designation distinguishes various shapes for a particular kind of material.

Tables 2. 3, and 4 present data on the static and dynamic stiffnesses. In Table 2 it is seen that the dynamic stiffness is always larger than the static stiffness. The static "end effect" should also be noted. If there was no end effect, changing the length of the mount by a factor of two should change the stiffness by a like factor. Comparing the static stiffness data for mounts 1C and 1D, it may be seen that changing the length by a factor of two results in a change in the stiffness by a factor of three and one-half. For longer mounts, such as 1A and 1B, the end effect is negligible.

TABLE 1

Physical Data for the Isolation Mounts Investigated Experimentally

Mount Designation	Length inches	Diameter inches	m pounds	Mount Material
1A	3.0	1.25	0.130	Soft rubber
1B	1.5	1.25	0.065	Soft rubber
1C	0.5	1.25	0.0217	Soft rubber
1D	0.25	1.25	...	Soft rubber
2A	3.97	1.25	0.204	Hard rubber
2B	1.96	1.25	0.101	Hard rubber
2C	0.51	1.25	0.0235	Hard rubber
2D	0.25	1.25	0.0134	Hard rubber
3	0.437	1.25	0.00274	Cell-tight rubber
4	...	...	0.178	Steel helical spring
5	0.73	1.25	0.0259	Corprene

TABLE 2

Comparison of Static and Dynamic Stiffness

The length of the mount is given in parentheses beside the mount designation. The frequency at which the dynamic stiffness was obtained is given in parentheses.

Mount	Static Stiffness lb/in.	Dynamic Stiffness lb/in.
1A (3 in.)	95	111 (27.5 cps)
1B (1.5 in.)	185	204 (37.5 cps)
1C (0.5 in.)	850	831 (80 cps)
1D (0.25 in.)	2800	3800 (150 cps)
2A (4 in.)	134	251 (44 cps)
2B (2 in.)	275	571 (64 cps)
2C (0.5 in.)	1140	3090 (145 cps)
2D (0.25 in.)	2600	18,000 (350 cps)

TABLE 3

Static Stiffness Versus Creep Time

Mount	Static Stiffness (1 sec creep)	Static Stiffness (30 sec creep)
2A (4 in.)	167	134
2B (2 in.)	310	275
2C (0.5 in.)	1400	1140
2D (0.25 in.)	5600	2600

The dynamic stiffness was then obtained through use of the equation $K=M\omega_0^2$. Table 4 presents the dynamic stiffness at different frequencies. The behavior of mount 2D is of interest. In Table 2 it is seen that mount 2D had the largest difference between static and dynamic stiffnesses. Now in Table 4, the dynamic stiffness of mount 2D is decreasing with decreasing frequency and is approaching the static value. These data are noteworthy since for the same material, save for a length of 4 in., there was no variation of the stiffness aside from the experimental; however, the frequency range was different. For the 4-inch mount (2A), the data presented in Figure 12 show that the elastic moduli are relatively constant for frequencies up to 1000 cps. Since this contradicts the data presented in Table 4 on the 0.25-inch mount (2D), the difference is quite possibly associated with the "end effect."

TABLE 4

Dynamic Stiffness Versus Frequency

Mount 1D	
Frequency cps	Stiffness lb/in.
32.5	3980
50.0	2710
87.5	3220
157	3800
Mount 2D	
41	6340
116	14,500
192	15,500
340	18,000

TABLE 5

Comparison of Computed and Measured Ratio of Standing Wave Frequency to the Low Resonant Frequency

Computed	Measured	Percent Error	Mount Designation	Mount Material
10.8	11.3	+4.6	1A	Soft rubber
14.7	16.3	+10.9	1B	Soft rubber
24.0	33.7	+40.5	1C	Soft rubber
8.22	8.90	+8.3	2A	Hard rubber
11.9	13.2	+11.0	2B	Hard rubber
36.0	43.0	+16.0	3	Cell-tight rubber
9.0	9.6	+6.7	4	Helical spring

Table 5 presents a comparison between the computed value of the ratio of the standing wave angular frequencies to the low resonant angular frequency ω_i/ω_0 and the experimentally measured value. It is to be noted that while the agreement is reasonably good, the experimental value always exceeds the computed value. This point is discussed further in the Appendix.

Table 6 presents the experimentally measured value of the dimensionless damping parameter n. It is to be noted that n is substantially constant for a reasonably wide frequency range, but tends to slowly increase. It is to be noted that at specific frequencies, the values of n given in Table 6 are smaller for short mounts than for longer mounts of the same material. This is a consequence of the rubber-metal bond which gives what has been referred to in this paper as the "end effect."

Consider a rubber cylinder bonded to two infinitely stiff objects, designated by M. Now the shear stress is given by $\tau_{xy} = 1/2(\sigma_x - \sigma_y)$ since the principal axes are chosen to coincide with coordinate axes x and y. At great distances from the constrained ends σ_y is nearly zero, and the shear stress is a maximum. Near the constrained ends σ_y approaches $\nu\sigma_x/1 - \nu$, and the shear stress decreases from its maximum value. Since the dissipation is proportional to the time rate of shear strain, the "end effect" results in a decrease of n.

There seems to be an equivalent point of view for seeing how this reduction of n because of the end effect comes about. Since $n = \omega\mu'/2E$ for a long thin cylinder, it is reasonable to expect that for more complicated cases E should be replaced by an effective modulus for the particular region in the material. Now we have seen in the Appendix that near the ends the effective modulus is larger than E and hence n is decreased.

TABLE 6

Values of the Damping Parameter n at the Resonant Frequencies

The mode number of the standing wave is designated by the subscript attached to the damping parameter n. The frequency in cycles per second is stated in parentheses beside the measured values of n.

n_0	n_1	n_2	Mount Designation	Mount Material
0.025 (27.5)	0.070 (310)	0.14 (570)	1A	Soft rubber
0.031 (37.5)	0.060 (610)	0.09 (1050)	1B	Soft rubber
0.036 (80.0)	...	...	1C	Soft rubber
0.079 (44)	0.120 (400)	0.140 (800)	2A	Hard rubber
0.090 (65)	0.11 (80)	...	2B	Hard rubber

Figures 8 - 10, inclusive, present transmissibility and phase curves for the various mounts whose data have been summarized in the preceding tables.

In Figures 8 - 10, inclusive, the theoretical curves based upon the measured values of n are superimposed upon the experimental curves. As may be seen, the agreement is quite good. The theoretical curves were computed on the assumption of constant velocity, which in turn implies a constant effective modulus. The agreement indicates that, as a first approximation, this is a good assumption on which to predict the performance of a vibration mount.

It is of interest to note in Table 5 the agreement between the computed and measured values of ω_i/ω_0 for the helical spring. It may seem surprising that, knowing the mass ratio M/m and the low resonance angular frequency ω_0, one is able to predict the standing wave frequency without knowing either the stiffness or the velocity of the elastic wave in the spring. A critical examination of the ways in which the mass ratio M/m was introduced as a parameter reveals that all this information is contained in its value.

Phase measurements were made, because it was found in some instances that this afforded a more sensitive method of detecting standing

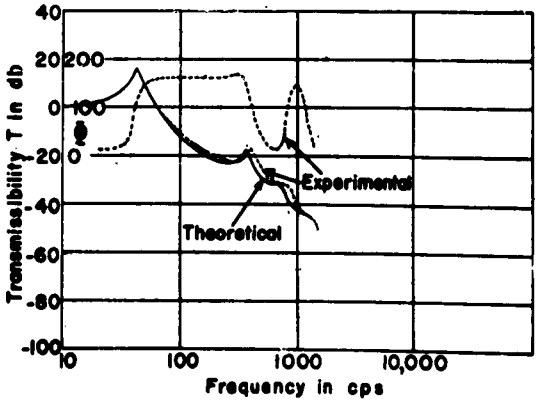

Figure 8 - Superposition of Theoretical and Experimental Curves of Transmissibility T in db and Phase in degrees versus Frequency in cps

Mount 1A, $M/m = 10.9$

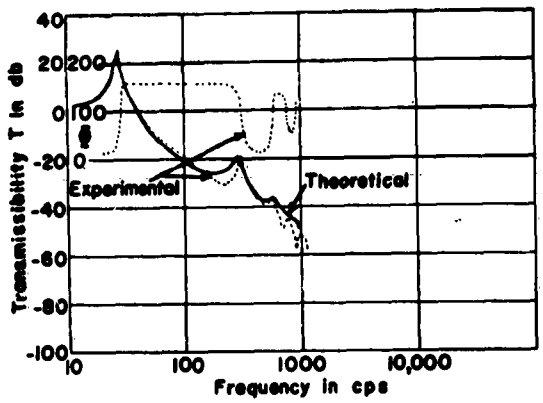

Figure 9 - Superposition of Theoretical and Experimental Curves of Transmissibility T in db and Phase in degrees versus Frequency in cps

Mount 1B, $M/m = 21.8$

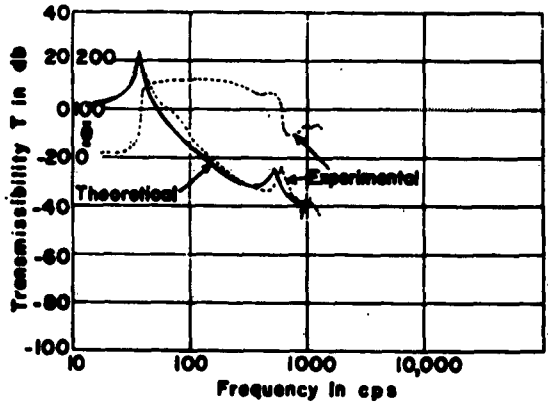

Figure 10 - Superposition of Theoretical and Experimental Curves of Transmissibility T in db and Phase in degrees versus Frequency in cps

Mount 1C, $M/m = 58.3$

wave frequencies than the transmissiblity. The phase is 90 degrees whenever a longitudinal standing wave occurs. Inspection of the experimental data reveals the characteristic behavior of the phase shifts associated with the standing waves.

MEASUREMENTS AND INSTRUMENTATION

The transmissibility T is defined as the ratio of the force F_B, which the isolation mount delivers to a base that consists of a rigid infinite mass, to the exciting force F applied to the machine. We shall view the system of the mass M plus the isolation mount as a four-terminal network a-b-c-d, as represented in Figure 11, where G is the vibration generator and Z_m is the impedance of the machine. The transmissibility is given by

$$T = \frac{F_{0c}}{F}$$

where F_{0c} is the open circuit force at terminals c-d, which correspond to a base of very high impedance.

It is convenient to use a theorem that simplifies the measurement problem. This theorem says the transmissibility is given by

$$T = \frac{V_{ac}}{V}$$

where V is the velocity at terminals c-d, and V_{ac} is the short circuit velocity at terminals a-b.

Also, it is true that the ratio of accelerations is identical with the ratio of velocities, since simple harmonic motion has been assumed.

The meaning of this exceedingly useful theorem is that instead of measuring forces when determining the transmissibility, one can measure the acceleration with accelerometers. The latter measurement is considerably simpler.

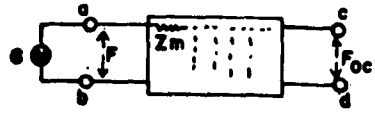

Figure 11- Representation of Isolation Mount and the Machine as a Four-Terminal Network

The proof of the theorem is as follows:

If terminals c-d are shorted, by Thevenin's theorem a velocity $V' = F_{oc}/Z_{cd}$ will result. Z_{cd} is the impedance measured between terminals c-d. Now if terminals a-b are short circuited and the generator is applied to terminals c-d, this is equivalent to applying a force $F' = VZ_{cd}$ to the terminals. Also, a velocity V_{ab} will appear at terminals a-b. Now by the reciprocity theorem,

$$\frac{V_{ab}}{F'} = \frac{V'}{F}$$

If the substitutions $V' = F_{oc}/Z_{cd}$ and $F' = VZ_{cd}$ are made, one obtains

$$T = \frac{F_{ab}}{F} = \frac{V_{ab}}{V} \qquad Q.E.D.$$

A block diagram of a simple measurement system is shown in Figure 12.

The vibration generator must be carefully adjusted to assure only vertical motion of the generator. The isolation mount is then stud-bolted in place and Massa accelerometers, Model 127, are secured in positions 1 and 2 as indicated.

The vibration generator is then driven by an oscillator-power amplifier combination at any desired frequency, and the amplitude and phase relationships of the outputs from the two accelerometers are measured. The difference in the amplitude readings measured in decibels relative to an arbitrary reference voltage gives the modulus of the transmissibility in decibels, and the phase measurement gives the phase angle of the transmissibility.

The signal to noise ratio was improved by using a General Radio, Model 736A, 4-cycle, band-width analyzer to make the measurements, both of amplitude and phase. Unfortunately, the analyzer is difficult to tune and must be calibrated frequently if accurate data are to be obtained. To facilitate the measurements, a system was devised for providing a signal to drive the power amplifier, to which the analyzer is automatically tuned. This greatly simplified the work, and it became evident that if a device could be

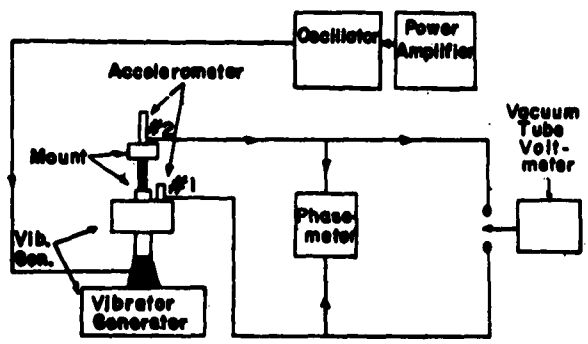

Figure 12 - Diagram of Simple Measuring System for the Testing of Isolation Mounts

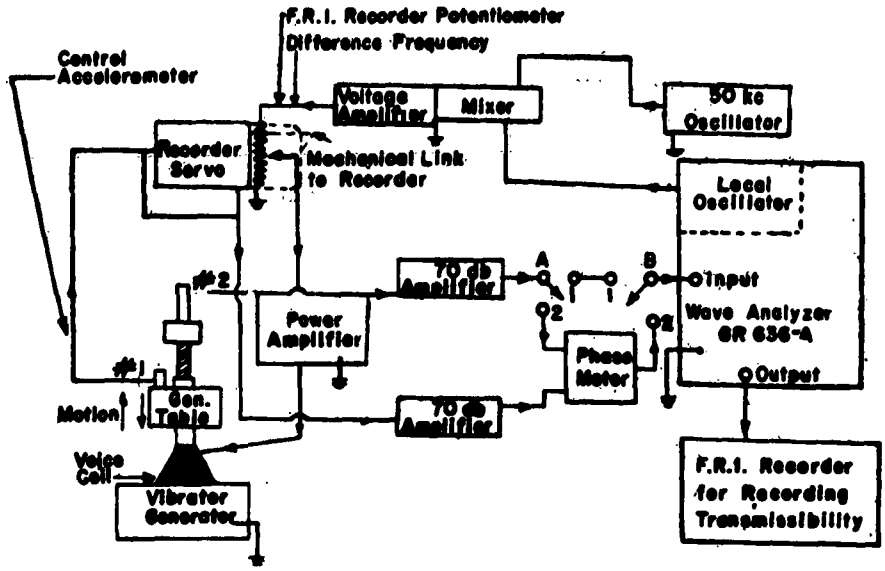

Figure 13 - Diagram of Complete Measuring System Incorporating a Servomechanism for Maintaining Constant Acceleration

1. To measure transmissibility amplitude, switches A and B must be in position 1.
2. To measure transmissibility phase, switches A and B must be in position 2.

constructed which would provide a constant acceleration output from the generator, direct recordings of transmissibility would be possible. Such a device was constructed, utilizing the servomechanism of an FR-1 recorder. The block diagram of the entire system is shown in Figure 13.

The phase meter is a system of comparing voltages by the voltage vector triangle method. It is possible to make measurements of phase between undistorted signals in the range from 50 to 10,000 cps to an accuracy greater than ± 1 degree for angles between 0 and 180 degrees. In principal, the same accuracy can be obtained by using the analyzer as a voltmeter for badly distorted signals. The phase meter accuracy is limited by the accuracy with which the voltage readings can be taken.

ENGINEERING IMPLICATIONS

In discussing how the experimental results bear on the problem of designing an isolation mount, the narrow viewpoint is adopted that noise reduction is the only goal. All other considerations, such as shock, damage, etc., are neglected. In other words, the discussion is limited to that of a machine that is subject to no outside influence, and the sole problem is to isolate the noise that is generated when the machine runs from the foundation

upon which the machine is sitting.

The importance of high damping has been noted elsewhere. The desirability of high damping is clearly indicated. If the damping is prescribed by some condition, the shape of the mount may still be varied. It is clear from the theoretical curves that if the low resonant angular frequency ω_e is specified, a large mass ratio M/m is desirable. This means that both the length and the cross-sectional area of the mount should be as small as possible. But there is a limit as to how small the area S can be. Because of the weight M_g of the machine, a strain is caused in the mount material that is given by

$$\text{strain} = \frac{M_g}{ES}$$

where E is the modulus of the material. There is a maximum permissible value for this strain because of considerations of creep, strength, etc. When the mount material is specified along with this value of maximum strain, then the minimum value of S is specified. Now since the stiffness K is given by

$$K = \frac{ES}{l}$$

and since ω_e and M are specified, K is specified. Then l is also specified, since S is given by the maximum permissible strain specification. Furthermore, this value of l is the minimum value under the circumstances. The preceding argument is perfectly consistent with another way of thinking about the matter. If the objective were to increase the standing wave frequencies to a high value, then one would minimize l. If ω_e and M, and hence K, were specified, then ES would be minimized, since l is minimized. However, in minimizing ES, the maximum strain specification must be observed, and thus the same conclusion is reached.

ACKNOWLEDGMENT

Acknowledgment is made to Mr. Murray Strasberg of the Bureau of Ships who not only formulated this problem but made substantial contributions to most of the ideas used in prosecuting the problem.

APPENDIX

THE VELOCITY OF COMPRESSION WAVES IN CYLINDRICAL MOUNTS AND THE END EFFECT

It was noted earlier that certain approximations were made in deriving the basic differential equation. The more exact theory is discussed elsewhere.[6] This reference shows that when the wavelength becomes an appreciable fraction of the diameter of the cylinder, there results a decrease in velocity from the value given by $C_0 = (E/\rho)^{1/2}$. To a first approximation this decrease in the velocity is caused by the radial motion. The inertia associated with this radial motion was neglected in the derivation[5] of the wave equation. If it is included it can be thought of as an increase of the denominator of the expression $C_0 = (E/\rho)^{1/2}$, and hence, it results in a decrease in velocity. Figure 14 presents the velocity dispersion curve. The abscissa is the ratio of diameter to wavelength, and the ordinate is the ratio of actual velocity to C_0.

Other approximations that affect the velocity have been made. Small damping was assumed to obtain Equation [6]. If such an assumption had not been made, the phase velocity of the wave would have been approximately $C \cong C_0 (1 + n^2/2)$.

There is still another approximation that is important. Near the ends of the cylinder that are bonded to the relatively stiff metal blocks the effective modulus of the material increases. As already noted in Table 2, this results in an increase in effective modulus. Figure 15 presents some typical data for the effective modulus of cylinders with varying length to diameter ratios. It is easily seen that the "end effect," which is associated with the rubber-metal bond, results in a higher effective modulus for the rubber. What is not so easily seen is that it has a different influence upon both the low frequency resonant waves and the standing waves. In Table 3 it was shown that the observed value of ω_1/ω_0 was always larger than the computed value. It will now be shown that this could be a consequence of the "end effect" having a different influence upon the low resonant frequency and the standing wave frequencies.

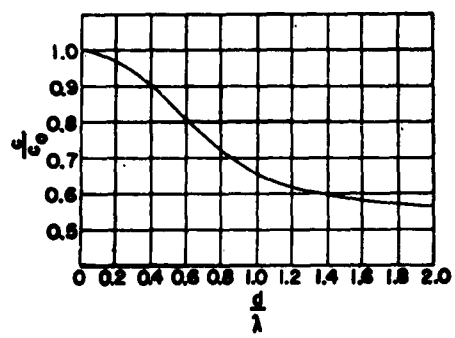

Figure 14 - Ratio of Longitudinal Wave Velocity in a Circular Cylinder to the Young's Modulus Velocity As a Function of Diameter to Wavelength Ratio d/λ

Consider a mount constructed

of two materials of moduli E' and E'' as illustrated in Figure 16. The mount at the low frequency resonance can be thought of as having two stiffnesses K_1 and K_2, where $K' = 2E'S/l$ and a corresponding relation holds for K'' (l and S are the length and cross-sectional area of the mount). Now ω_0 will be given by $\omega_0 = (K/M)^{1/2}$, where $K = K'K''/(K'+K'')$. If one then attempts to compute the velocity based on the measured values of M and by means of the equation

$$C_0 = \left(\frac{E}{\rho}\right)^{1/2} = \left(\frac{Kl}{\rho S}\right)^{1/2}$$

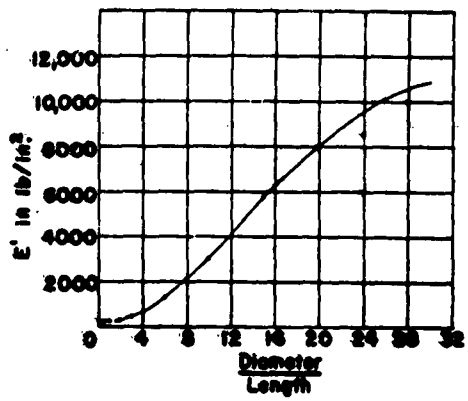

Figure 15 - Effective Modulus versus Diameter to Length Ratio for a Circular Cylinder with Constrained Ends

a misleading answer is obtained, as will now be shown.

The velocity C_1, which determines ω_1, the standing wave angular frequency, is the average velocity for the entire length of the mount. It will now be demonstrated that C_1 is always larger than C_0.

The velocities in the different parts of the mount are

$$C' = \frac{l}{2t'}$$

$$C'' = \frac{l}{2t''}$$

where t' and t'' are the times required by the wave to travel through the different parts of the mount. Now the velocity C_1 is

$$C_1 = \frac{l}{(t'+t'')}$$

Substituting the previous expressions for C' and C'' gives

$$C_1 = 2\frac{C'C''}{C'+C''}$$

Writing this in terms of the moduli E' and E'', one obtains

$$C_1 = \frac{2}{\rho^{1/2}} \frac{(E'E'')^{1/2}}{E'^{1/2}+E''^{1/2}}$$

Figure 16 - Diagram of an Isolation Mount Constructed of Two Materials of Differing Young's Modulus E' and E''

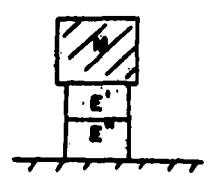

Writing C_0 in terms of E' and E'' gives

$$C_0 = \left(\frac{2}{\rho}\right)^{1/2} \frac{(E'E'')^{1/2}}{(E'+E'')^{1/2}}$$

Consider now the ratio C_1/C_0. This is

$$\frac{C_1}{C_0} = 2^{1/2} \frac{(E'+E'')^{1/2}}{E'^{1/2}+E''^{1/2}}$$

and is clearly larger than unity, except when $E' = E''$, in which case it becomes equal to unity. All the theoretical curves and standing wave frequencies are computed on the basis of constant velocity of the wave in the mount where the velocity is based upon data obtained at the low frequency resonance. Hence, it is to be expected that there will be discrepancies of the type observed in Table 5.

This special case follows from a more general theorem that is not yet ready for publication.

To summarize, the velocity of the elastic wave in a compression mount with constrained ends is subject to three influences. The velocity will tend to decrease with increasing frequency because of the radial motion. The value of the damping parameter n tends to increase with increasing frequency, and this results in an increase in velocity. The "end effect" results in an effective increase in velocity with increasing frequency. These three influences co-exist and make a precise prediction of the variation of velocity with frequency exceedingly difficult.

REFERENCES

1. Hartog, Den, "Mechanical Vibrations," McGraw-Hill Book Company, Inc., New York, 1940.

2. Illinois Institute of Technology Engineering Report No. 2, "Resilient Mountings for Reciprocating and Rotating Machinery," ONR Contract N7-onr-32904.

3. Rayleigh, Lord, "The Theory of Sound," Dover Publications, New York, 1945.

4. Nolle, A.W., "The Acoustic Determination of the Physical Constants of Rubber-like Material," J. Acoust. Soc. Am., Vol. 19, 1947, pp. 194-201.

5. Slater, J.C., "Microwave Transmission," McGraw-Hill Book Company, Inc., New York, 1942.

6. Hudson, G.E., "Dispersion of Elastic Waves in Solid Circular Cylinders," Phys. Rev., Vol. 63, 1943, pp. 46-51.